
Study of Structural and Mechanical Properties of the Transparent Bismuth Borate Glass Ceramic

Pushpinder Singh, Dr. JD Sharma

Department of Materials and Metallurgical Engineering

Punjab Engineering College, Chandigarh, India

ABSTRACT

Structural and mechanical properties of the photocatalytic transparent $2\text{Bi}_2\text{O}_3\text{-B}_2\text{O}_3$ glasses were studied. X-ray diffraction substantiated the presence of photocatalytic $\text{Bi}_4\text{B}_2\text{O}_9$ crystals embedded in the glass matrix of bismuth borate glass ceramics heat treated for 2 hr, 3 hr, 4 hr, 5 hr and 6 hr at 400°C . The size of $\text{Bi}_4\text{B}_2\text{O}_9$ crystals decreased with the increase in the time of heat treatment. Fourier transform infrared spectroscopy revealed the bending vibration of B-O-B bonds in (BO_3) triangle, vibration of Bi-O-Bi in (BiO_6) octahedron, stretching vibration of (BO_4) tetrahedron, stretching vibrations in BiO_6 units and stretching vibration of (BO_4) tetrahedron. Microhardness of the heat treated glass demonstrated the increasing trend with the increase in the time of heat treatment.

keywords-BBO, glass ceramic, optical transparent, photocatalytic glass ceramic, transparent glass.

1. INTRODUCTION

Now a day, promoting clean energy initiatives and urge for eco-friendly innovative materials for their use in the present day world have brought the researchers from all around the world on the common ground to develop eco-friendly innovative materials which is simple to fabricate with sufficient mechanical and chemical properties and economically viable. These materials are now the need of the hour. The glass ceramics are one of them.

Various authors exhibited that a number of photocatalyst have been developed either in the powder form or thin film or the photocatalytic crystals embed in the matrix [1-3]. These photocatalyst came into existence as efficient and economically viable in the clean energy and environment applications. Since the finding of TiO_2 as photocatalyst it has been extensively used as photocatalyst [4-8].

Huang et al. revealed that $\text{Bi}_2\text{O}_2\text{CO}_3$ tuned with carbonate ion possess satisfactory photocatalytic properties [9]. Huang et al. also exhibited that $\text{Bi}_4\text{B}_2\text{O}_9$ crystals showed satisfactory photocatalytic properties and $\text{Bi}_4\text{B}_2\text{O}_9$ was formed using the solid state reaction. He also observed degradation of methylene blue under simulated solar irradiation [10].

Sharma et al. found that $\text{Bi}_4\text{B}_2\text{O}_9$ crystals embedded in the glass matrix prepared by the melt quenching technique showed satisfactory photocatalytic activity along with the photo induced hydrophilicity thereby making the transparent glass ceramics use in the self-cleaning application [11].

Authors have exhibited that glass ceramics have been used as a photocatalyst to treat waste water. [12-13].

Authors have also identified glass and glass-ceramics as key elements to most of the great engineering advancements of the 20th century, following the development of solid state lasers and optical glass fibers, biomaterials, glasses for imaging technologies, glass films in microelectronic devices [14]. Glass and glass ceramics being a structural material have found to be having inherent advantages such as low cost, easy to fabricate, transparency, mechanical and chemical stability. Glass-ceramics contain crystallites in the amorphous matrix and possess some additional properties.

Glass-ceramics were discovered in 1953. Since then, a lot of research papers have been published on glass-ceramics by research institutes, and varsities.

Glass-ceramics are mostly produced in two steps: In First step, a glass is formed by a glass-manufacturing process. The glass is cooled down and is then reheated in a second step. In this heat treatment the glass partly crystallizes. Glass-ceramics are produced by controlled crystallization of glasses with addition of nucleating additives, in most cases nucleation agents (e.g., noble metals, fluorides, ZrO_2 , TiO_2 , P_2O_5 , Cr_2O_3 or Fe_2O_3) are added to the base composition of the glass-ceramic in contrast to a spontaneous crystallization, which is not wanted in glass manufacturing. These nucleation agent aids and control the crystallization process. They always contain a residual glassy phase and one or more embedded crystalline phases. Controlled crystallization gives an ordered series or arrangement of crystals in the materials with interesting combinations of properties. Glass-ceramics are vested with the fabrication advantage of glass, as well as special properties of ceramics.

Therefore, towards the study of photocatalytic transparent bismuth borate based glass ceramics, we have selected the composition of $2Bi_2O_3-B_2O_3$ (BBO) having borate oxide which is one of the good glass formers. In the present work, $2Bi_2O_3-B_2O_3$ (BBO) transparent glass ceramics have been fabricated to have photocatalytic $Bi_4B_2O_9$ crystals and their inherent and mechanical properties have been studied.

2. Experimental

$2Bi_2O_3-B_2O_3$ (BBO) glasses were fabricated using the conventional melt-quenching method. For glass preparation, Bi_2O_3 and B_2O_3 were weighed and ball milled for 1 hour at 1000 rpm. Table.1 depicts the chemical composition of Bi_2O_3 and B_2O_3 in gm.

Table 1. Chemical composition of glass sample

material	Chemical Composition in gm
Bi_2O_3	9.3063
B_2O_3	0.6937

After homogeneous mixing, a batch of 10 g was used for melting in alumina crucible in the furnace at $1000^\circ C$ for 1 hour. After melting, the melt was poured onto a stainless steel plate preheated up to $250^\circ C$ and was flattened with another steel plate maintained at the same temperature. The details of processing parameters are shown in Table 2.

Table 2. List of processing parameters for preparation of glass sample

Ball milling time	1 h
Ball milling speed	100 rpm
temperature in furnace	$1000^\circ C$
Holding temperature in furnace	1 h
Preheat temperature of lower plates	$250^\circ C$
Preheat temperature of upper plates	$250^\circ C$
Type of crucible	25 ml alumina

Stainless steel 304 grade plates of dimension $150 \times 70 \times 8$ mm each have been used for the base and upper part of the setup. Each plate has been subject to grinding, buffing and polishing process so that the surface of the glass formed would be of high finish.

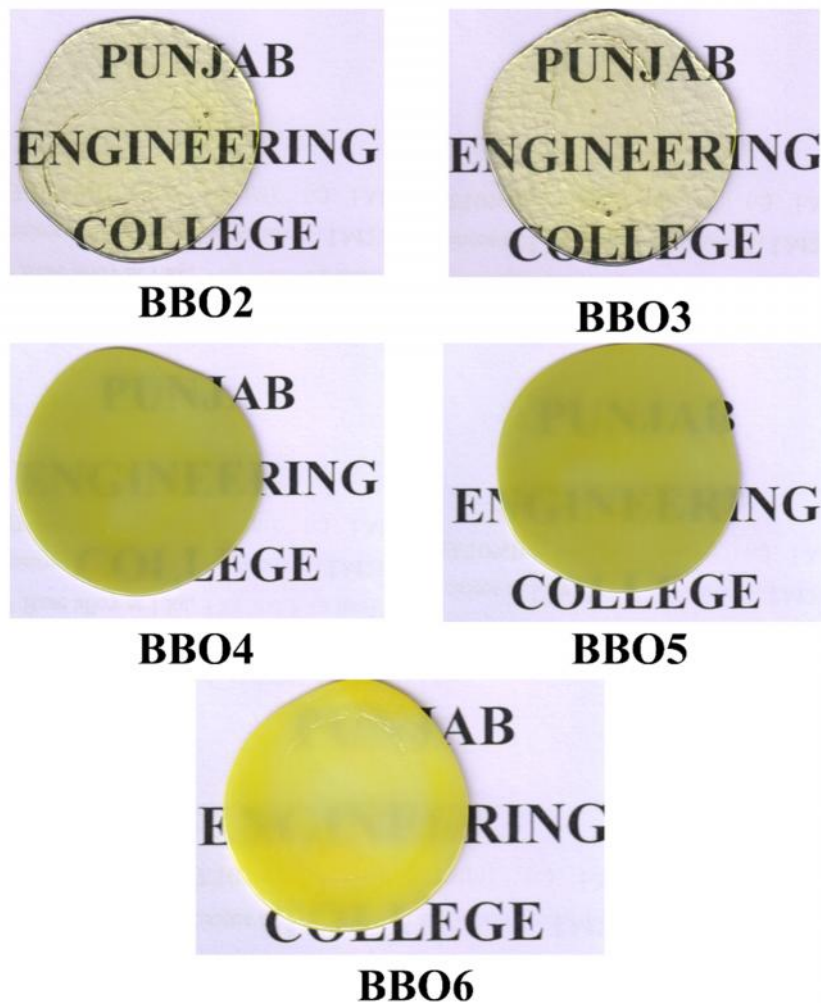


Fig.1 Optical images of the BBO glass ceramic (a) BBO2, (b) BBO3, (c) BBO4, (d) BBO5, (e) BBO6.

3. CHARACTERIZATION AND TESTING DETAILS

The heat treated samples were Characterised by X-ray diffraction PANalytical (Cu K₁ radiation $\lambda = 1.54 \text{ \AA}$, 40 mA, 45 kV) at a scanning rate of 2° per min, Step Size 2 equal to 0.0170 with 2 θ ranging from 10.008° to 89.9934°. Crystallization was controlled by heat treating (HT) the samples at 380°C for 2 hr, 3 hr, 4 hr, 5 hr and 6 hr which have been referred in the manuscript as BBO2, BBO3, BBO4, BBO5, BBO6 respectively as shown in the fig.1. FTIR PerkinElmer was used to perform Fourier transform infrared spectroscopy of the samples under study. Microhardness values were measured using Vickers hardness testing machine. Microhardness was performed at room temperature using the square-based pyramid diamond indenter.

4. RESULTS AND DISCUSSION

4.1 Crystal size of the photocatalytic Bi₄B₂O₉ crystals

Fig.2 shows the XRD patterns of crystallized samples where sharp peaks mark the presence of micro/nano crystallites and all peaks in the heat-treated samples have been matched with the Bi₄B₂O₉ crystals (JCPDS card No.01070-1458).

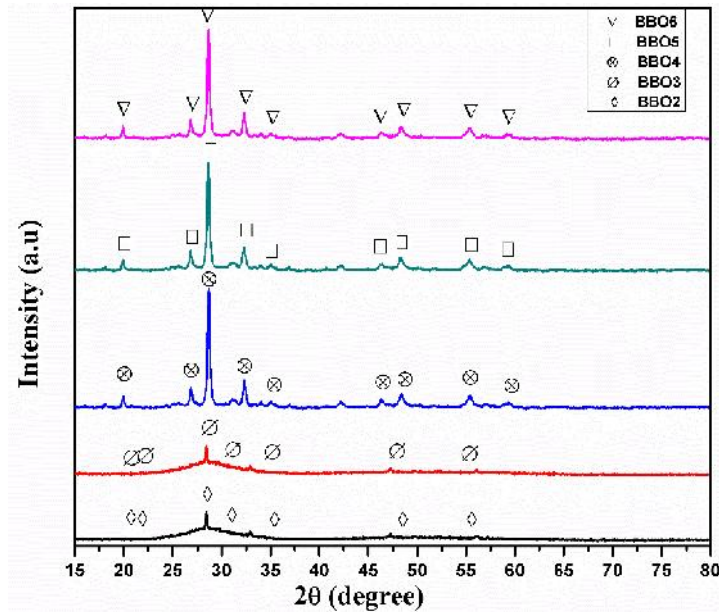


Fig.2 XRD patterns of the heat treated glass sample.

$\text{Bi}_4\text{B}_2\text{O}_9$ crystals size is calculated by the Scherrer equation. It is a formula that relates the size of crystallites, in a solid to the broadening of a peak in a diffraction pattern. It is used in the determination of size of particles of crystals in the form of powder.

The Scherrer equation can be written as:

$$D = \frac{k\lambda}{\beta \cos\theta} \quad (1)$$

Where, θ is the Bragg angle. k is the constant of proportionality, k (the Scherrer constant) depends on the how the width is determined, the shape of the crystal, and the size distribution.

k actually varies from 0.62 to 2.08 is a dimensionless shape factor, with a value close to unity. The shape factor has a typical value of about 0.9, but varies with the actual shape of the crystallite. λ is the X-ray wavelength. Full Width at Half Maximum (FWHM) –the width of the diffraction peak, in radians, at a height half-way between background and the peak maximum is the line broadening at half the maximum intensity (FWHM). D is the mean size of the crystallite domain.

Calculation of the mean crystallite domain for BBO2 by taking observed bragg angle and the FWHM values at the corresponding bragg angles and thereby the size of the crystal domain is calculated by the scherrer formula as shown in (1). The observed angle varied from 20.849° to 55.686° . The size of the crystal domain varied from 68.1796 nm to 146.7470 nm and the average size of the crystal have been found out to be 100.0613875 nm for BBO2 glass ceramic.

Similarly, Calculation of the mean crystallite domain for BBO3 by taking observed bragg angle and the FWHM values at the corresponding bragg angles. The observed angle varied from 20.849° to 55.686° . The size of the crystal domain varied from 60.2273 nm to 146.7470 nm and the average size of the crystal have been found out to be 98.6968 nm for BBO3 glass ceramic.

For BBO4, the observed angle varied from 19.914° to 59.402° . The size of the crystal domain varied from 11.20382 nm to 40.1787 nm and the average size of the crystal have been found out to be 26.4431 nm for BBO4 glass ceramic. For BBO5, the observed angle varied from 19.888° to 59.341° . The size of the crystal domain varied from 9.33369 nm to 33.4800 nm and the average size of the crystal have been found out to be 22.533063 nm for BBO5 glass ceramic.

For BBO6, the observed angle varied from 28.661° to 59.322° . The size of the crystal domain varied from 12.62671 nm to 36.52514 nm and the average size of the crystal have been found out to be 21.5514 nm for BBO6 glass ceramic.

Fig .3 shows the decreasing trend in average crystal size with the increase in the time of heat treatment. More the time of heat treatment more is the rate of nucleation. It can be attributed from the results that nucleation rate increased at a very fast rate after 3 hr. However, the difference in rate of nucleation for 4 hr, 5 hr and 6 hr was approximately the same. Hence it is evident from the X ray diffraction results of the bismuth borate glass ceramic that there is presence of micro to nano photocatalytic $\text{Bi}_4\text{B}_2\text{O}_9$ crystals embedded in the BBO glass host matrix.

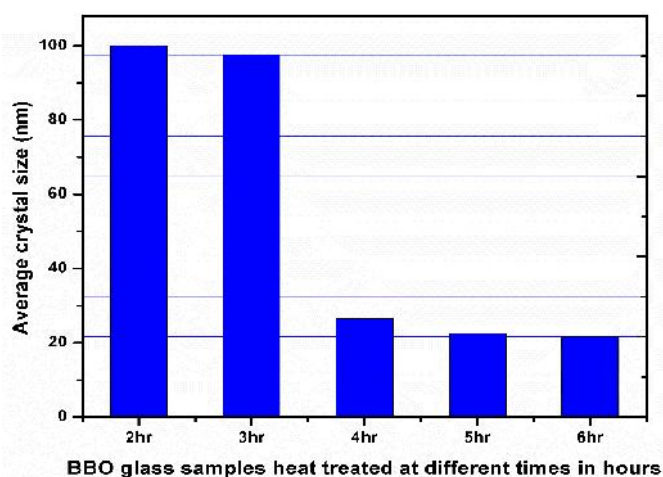


Fig. 3 Variation of average crystal size with time

4.2 FTIR spectra of the heat treated glass samples

Figure 4 shows atomic vibrational modes examined by FTIR spectroscopy. Usually, the atomic vibrations in all bismuth borate glasses show almost similar pattern. Cheng et al. performed the structural investigations of $\text{Bi}_2\text{O}_3\text{-B}_2\text{O}_3$ glasses using infrared spectroscopy [15]. Stone et al. have found asymmetric B-O bonds for the BO_3 and BO_4 coordination in the $\text{Bi}_2\text{O}_3\text{-B}_2\text{O}_3$ glass system [16]. Hyman et al. examined the crystal structure using X-ray diffraction and showed that BO_3^{3-} anions are arranged in discrete planes and held in coordination with bismuth atoms [17]. In the case of $\text{Bi}_2\text{O}_3\text{-B}_2\text{O}_3$ glass sample sharp peaks in band $(420\text{--}576)\text{ cm}^{-1}$ correspond to the vibration of Bi-O-Bi in BiO_6 octahedron [18-19]. A sharp band at $(590\text{--}725)\text{ cm}^{-1}$ is due to B-O-B bending vibrations in BO_3 triangular units [20]. The sharp band at $(750\text{--}1000)\text{ cm}^{-1}$ with a shoulder represents the symmetric bonds stretching of B-O in (BO_4) tetrahedral units. [18,20]. The shoulder belonging to another broad band at $1031\text{--}1326\text{ cm}^{-1}$ is due to symmetric stretching of B-O-B in BO_3 triangles under BO_4 coordination [18,21]. Similarly, bands at $1350\text{--}1600\text{ cm}^{-1}$ belong to asymmetric stretching relaxation of the B-O bonds in tetrahedral BO_4 coordination. FTIR results shows the well coordination of B-O-B linkages. Table 3 shows the FTIR bands assigned for heated glass samples.

Table 3. Assignment of FTIR bands spectra analyzed in heat treated glass samples

Wavenumber (cm^{-1})	FTIR assignment
420–576	Vibration of Bi-O-Bi in $[\text{BiO}_6]$ octahedron
590–725	Stretching vibrations of Bi-O in BiO_6 units, bending vibration of B-O-B in $[\text{BO}_3]$ triangle
750–1000	Stretching vibration of $[\text{BO}_4]$ tetrahedron
1031–1326, 1350–1600	Stretching vibration of B-O-B in $[\text{BO}_3]$ triangles

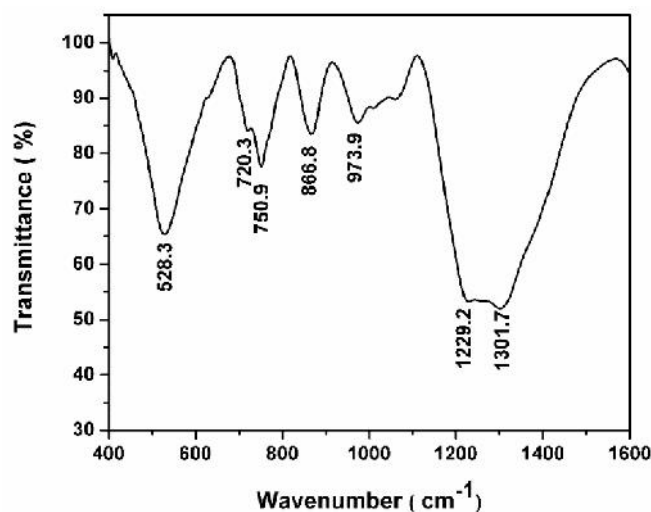


Fig.4 FTIR bands spectra observed in heat treated glass samples.

4.3 Microhardness studies

Microhardness was performed at room temperature using the square-based pyramid diamond indenter. For the better estimation of the surface hardness, each sample was subjected to indents at different positions by varying the load from 10gf to 100 gfor each indent so that indenter shape should be capable of producing geometrically similar pattern andhave well-defined points of measurement. At 100 gf geometrical impressions were fine and measuring points were clearly visible. The loading force of 100 gf, loading rate and dwell time were kept constant for all the samples understudy. Table 4 summarizes the hardness values obtained for BBO glass sample heat treated for 2 hr, 3 hr, 4 hr, 5 hr and 6 hr at 400°C. Fig 5 shows the variation of hardness value at different times.

Table 4. Hardness value of BBO glass sample at different times

Heat treatment time	Hardness (HV)				
	BBO2	BBO3	BBO4	BBO5	BBO6
2h	70	-	-	-	-
3h	-	89	-	-	-
4h	-	-	238	-	-
5h	-	-	-	277	-
6h	-	-	-	-	290

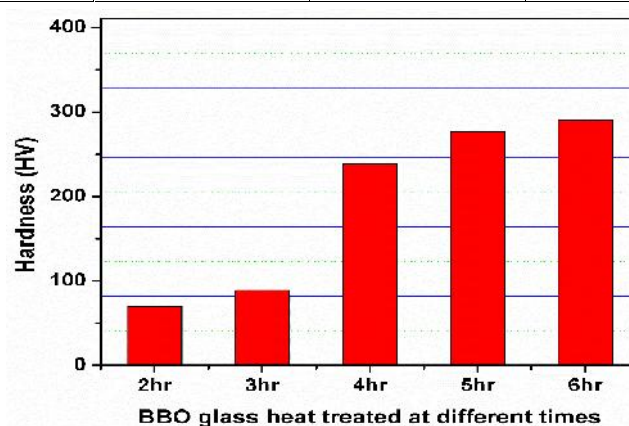


Fig.5Variation of the hardness of BBO glass sample at different time

5. CONCLUSIONS

The study of the effect of crystallization time on the structural and mechanical properties of the bismuth borate glass ceramic have shown the following results which are as follows:

1. Heat treatment of $2\text{Bi}_2\text{O}_3\text{-B}_2\text{O}_3$ glass ceramic at increasing order of time has resulted approximately 21-26 nm **photocatalytic** $\text{Bi}_4\text{B}_2\text{O}_9$ crystals in the $2\text{Bi}_2\text{O}_3\text{-B}_2\text{O}_3$ glass matrix.
2. Fourier transform infrared spectroscopy resulted well coordination of B-O-B linkages in BO_3 and BO_4 units.
3. Microhardness of the $2\text{Bi}_2\text{O}_3\text{-B}_2\text{O}_3$ glass ceramic have found to be increased with the increase in the heat treatment time.

REFERENCES

- [1] Kumar, S. G. and Devi, L. G.(2011).Review on Modified TiO_2 Photocatalysis under UV/Visible Light: Selected Results and Related Mechanisms on Interfacial Charge Carrier Transfer Dynamics. *J. Phys. Chem. A* 115, 46, 13211–13241.
- [2] Kabra, K., Chaudhary, R. and Sawhney, R. L. (2004).Review on treatment of Hazardous Organic and Inorganic Compounds through Aqueous-Phase Photocatalysis. *Ind. Eng. Chem. Res.* 43,24, 7683–7696.
- [3] McCullagh, C., Robertson, J. M.,Bahnmann,D. W. and Robertson P. K.(2007). Review on the application of TiO_2 photocatalysis for disinfection of water contaminated with pathogenic micro-organisms. *Res. Chem. Intermed.* 33, 359–375 (2007).
- [4] Kong, M., Li, y., Chen, X., Tian, T., Fang, P., Zheng,F. and Zhao X. (2011).Tuning the relative concentration ratio of bulk defects to surface defects in TiO_2 nanocrystals leads to high photocatalytic efficiency.*J. Am.Chem. Soc.* 133, 16414–16417.
- [5] Liqiang,J.,Xiaojun,S.,Baifu, X., Baiqi,W.,Weimin, C., and Honggang,F. (2004). The preparation and characterization of La doped TiO_2 nanoparticles and their photocatalytic activity. *J. Solid State Chem.* 177, 3375–3382.
- [6] Cassar,L.(2004). Photocatalysis of Cementitious Materials: Clean Buildings and Clean Air. *MRS Bull.* 29, 328–331.
- [7] Williams,G., Seger,B. and Kamat, P. V.(2008). TiO_2 -Graphene Nanocomposites. UV-Assisted Photocatalytic Reduction of Graphene Oxide.*ACS Nano* 2, 1487–1491.
- [8] Yu,J. C., Ho,W., Lin,J., Yip,H. and Wong,P. K.(2003).Photocatalytic activity, antibacterial effect, and photoinduced hydrophilicity of TiO_2 films coated on a stainless steel substrate. *Environ. Sci. Technol.*37, 2296–2301.
- [9] Huang,H.Li,X., Wang, J., Dong, F., Chu, P. K., Zhang, T., and Zhang, Y. (2015).Anionic Group Self-Doping as a Promising Strategy: Band-Gap Engineering and Multi-Functional Applications of High-Performance CO_3^{2-} -Doped $\text{Bi}_2\text{O}_2\text{CO}_3$.*ACS Catal.* 5, 7, 4094–4103.
- [10] Huang, H., He, Y., Lin, Z., Kang, L. and Zhang, Y. (2013).Two Novel Bi-Based Borate Photocatalysts: Crystal Structure, Electronic Structure, Photoelectrochemical Properties, and Photocatalytic Activity under Simulated Solar Light Irradiation. *J. Phys. Chem. C* 117,22986–22994.
- [11] Sharma, S. K., Singh, V. P.,Chauhan, Vishal S.,Kushwaha,H. S. and Vaish, R. (2017). Photocatalytic self-cleaning transparent $2\text{Bi}_2\text{O}_3\text{-B}_2\text{O}_3$ glass ceramics. *J. App. Phys.* 22, 094901.
- [12] Margha, F. H., Badawy, M. I. and Gad-Allah,T. A. (2017).ZnO enriched transparent glass ceramics for wastewater decontamination. *Environ. Prog.Sustainable Energy* 36, 442–447.
- [13] Kushwaha,H.,Parmesh, G., Vaish,R. and Varma.K. (2015). TiO_2 microcrystallized glass plate mediated photocatalytic degradation of estrogenic pollutant in water. *J. Non-Cryst. Solids* 408, 13–17.
- [14] Brow, R.K., Schmitt, M.L (2009). A survey of energy and environmental applications ofglass. *J. Eur. Ceram. Soc.* 29,1193–201.
- [15] Cheng,Y., Xiao,H. and Guo,W. (2008). Influence of rare-earth oxides on structure and crystallization properties of $\text{Bi}_2\text{O}_3\text{-B}_2\text{O}_3$ glass. *Mater. Sci. Eng. A* 480, 56–61.
- [16] Stone, C., Wright, A., Sinclair, R., Feller, S., Affatigato, M., Hogan, D., Nelson, N., Vira, C., Dimitriev, Y., Gattef, E. and Ehr, D. (2000).Structure of bismuth borate glasses. *Phys. Chem. Glasses*41, 409–412.

-
- [17] Hyman,A. and Perloff,A. (1972). The crystal structure of $2\text{Bi}_2\text{O}_3\text{-B}_2\text{O}_3$.Acta Crystallogr., Sect. B: Struct. Crystallogr.Cryst. Chem. 28, 2007–2011.
- [18] Cheng, Y., Xiao, H. and Guo,W. (2006). Structure and crystallization kinetics of $\text{Bi}_2\text{O}_3\text{-B}_2\text{O}_3$ glasses. Thermochem. Acta 444, 173–178.
- [19] Lines, M., Miller, A., Nassau, K. and Lyons,K. (1987). Absolute Raman intensity in glasses. J. Non-Cryst. Solids 89,163–180.
- [20] El-Damrawi,G. and El-Egili,K. (2001). Charaterization of novel $\text{CeO}_2\text{-B}_2\text{O}_3$ glasses, structure and properties. Phys. B: Condens. Matter 299, 180–186.
- [21] Kamitsos, E.,Patsis,A., Karakassides,M. and Chryssikos,G. D. (1990). Infrared reflectance spectra of lithium borate glasses. J. NonCryst. Solids 126, 52–67.